THE JOURNAL OF COMPARATIVE NEUROLOGY 461:452–465 (2003)

Axonal Pathways to the Lateral Superior Olive Labeled with Biotinylated Dextran Amine Injections in the Dorsal Cochlear Nucleus of Rats

JOHN R. DOUCET[1]* AND DAVID K. RYUGO[1,2]
[1]Department of Otolaryngology-Head and Neck Surgery, Center for Hearing Sciences, Johns Hopkins University School of Medicine, Baltimore, Maryland 21205
[2]Department of Neuroscience, Johns Hopkins University School of Medicine, Baltimore, Maryland 21205

ABSTRACT

The lateral superior olive (LSO) contains cells that are sensitive to intensity differences between the two ears, a feature used by the brain to localize sounds in space. This report describes a source of input to the LSO that complements bushy cell projections from the ventral cochlear nucleus (VCN). Injections of biotinylated dextran amine (BDA) into the dorsal cochlear nucleus (DCN) of the rat label axons and swellings in several brainstem structures, including the ipsilateral LSO. Labeling in the ipsilateral LSO was confined to a thin band that extended throughout the length of the structure such that it resembled an LSO isofrequency lamina. The source of this labeled pathway was not obvious, because DCN neurons do not project to the LSO, and VCN bushy cells were not filled by these injections. Filled neurons in several brainstem structures emerged as possible sources. Three observations suggest that most of the axonal labeling in the LSO derives from a single source. First, the number of labeled VCN planar multipolar cells and the amount of labeling in the LSO were consistent and robust across animals. In contrast, the number of labeled cells in most other structures was small and highly variable. Second, the locations of planar cells and filled axons in the LSO were related topographically to the position of the DCN injection site. Third, labeled terminal arborizations in the LSO arose from collaterals of axons in the trapezoid body (output tract of planar cells). We infer that planar multipolar cells, in addition to bushy cells, are a source of ascending input from the cochlear nucleus to the LSO. J. Comp. Neurol. 461:452–465, 2003.

Indexing terms: axon collaterals; binaural hearing; intensity coding; neuroanatomy

The lateral superior olive (LSO) is one of several distinct nuclei that form the superior olivary complex (SOC). The SOC is located in the upper medulla, rostral to the facial nucleus and flanked by the abducens and facial nerves. The LSO receives binaural input by way of the cochlear nuclei (CN) and so is part of an ascending pathway that is hypothesized to process sound localization cues (for reviews see Schwartz, 1992; Irvine, 1992). In turn, the axons of LSO principal neurons target cells in the nuclei of the lateral lemniscus and the inferior colliculus (Beyerl, 1978; Glendenning et al., 1981; Glendenning and Masterton, 1983). In rodents, such as the rat, the LSO also gives rise to descending pathways that end in the cochlea (White and Warr, 1983; Aschoff and Ostwald, 1988). Many LSO principal cells are sensitive to interaural intensity differences (IIDs), one of the acoustic features used to localize sounds in space (Boudreau and Tsuchitani, 1968; Goldberg and Brown, 1969; Caird and Klinke, 1983; Park et al.,

Grant sponsor: National Institutes of Health/National Institute on Deafness and Other Communication Disorders; Grant numbers: DC00232 and DC04395 (D.K.R.); Grant number: DC04505 (J.R.D.).

*Correspondence to: John R. Doucet, Center for Hearing Sciences, Johns Hopkins University School of Medicine, 720 Rutland Avenue, Baltimore, MD 21205. E-mail: jdoucet@bme.jhu.edu

Received 6 September 2002; Revised 11 February 2003; Accepted 19 February 2003

DOI 10.1002/cne.10722

Published online the week of May 19, 2003 in Wiley InterScience (www.interscience.wiley.com).

1997; Irvine et al., 2001; Tollin and Yin, 2002a,b). This sensitivity implies that LSO principal cells are targeted by neural pathways that encode intensity. In the present study, we provide evidence that planar cells, a subclass of multipolar cells in the ventral cochlear nucleus (VCN), project to the LSO.

The LSO receives input from two neural pathways that originate in each CN (Warr, 1966; van Noort, 1969; Tolbert and Morest, 1982; Glendenning et al., 1985; Cant and Casseday, 1986). Spherical bushy cells (SBCs) from the ipsilateral CN are thought to provide excitatory input to LSO neurons (Glendenning et al., 1985; Cant and Casseday, 1986; Smith et al., 1993). Globular bushy cells (GBCs) initiate the pathway beginning on the opposite side of the brain. GBCs project to the contralateral medial nucleus of the trapezoid body (MNTB; Tolbert and Morest, 1982; Spirou et al., 1990; Smith et al., 1991), and MNTB neurons then send inhibitory projections to the LSO on the same side (Spangler et al., 1985; Kuwabara and Zook, 1991; Smith et al., 1998; Henkel and Gabriele, 1999; Sanes and Friauf, 2000). The two inputs create EI cells that are excited by sounds in the ipsilateral ear and inhibited by sounds in the contralateral ear. EI cells vary with respect to the range of IIDs causing changes in their discharge rate. Because LSO cells are sensitive to IIDs over a wide range of average intensities (Boudreau and Tsuchitani, 1968; Goldberg and Brown, 1969; Tsuchitani, 1977; Tollin and Yin, 2002a), the two pathways converging in the LSO are hypothesized to signal changes in intensity even at high intensities. Intensity coding in the auditory nerve and the CN remains a key question impacting models of spectral representation, signal detection in noise, as well as sound localization. Therefore, resolving the pathways and mechanisms underlying the sensitivity of LSO cells to IIDs is crucial for a better understanding of the mechanisms for intensity coding at these early stages of the auditory pathway.

The direct and indirect innervation of the LSO by VCN bushy cells is well documented, but there is also evidence that other VCN cell types project to the LSO. Retrograde and anterograde tracing techniques have demonstrated that neurons in the posterior VCN (PVCN) project to the ipsilateral LSO (Glendenning et al., 1985; Cant and Casseday, 1986; Thompson and Thompson, 1987, 1991; Vater and Feng, 1990; Thompson, 1998). Multipolar (stellate) cells are the dominant cell class in this division of the VCN, whereas most bushy cells are located in the anterior VCN (AVCN) or rostral PVCN (Cant, 1992). In addition, a few examples of intracellularly filled multipolar cells have been observed to send a collateral axon into the ipsilateral LSO (Rouiller and Ryugo, 1984; Friauf and Ostwald, 1988). Multipolar cells are composed of distinct subclasses of neurons, and the particular groups that innervate the LSO are unknown.

We have been studying the morphology and axonal projections of VCN multipolar cells (Doucet and Ryugo, 1997; Doucet et al., 1999b). In these studies, multipolar neurons were retrogradely labeled after making a small injection of biotinylated dextran amine (BDA) into the DCN. In the same experiments, we noticed a prominent band of anterogradely filled axons and swellings in the ipsilateral LSO. Because DCN neurons do not innervate the ipsilateral LSO (Osen, 1972; Warr, 1982), we sought to identify the source of these filled axons. We analyzed the number and location of retrogradely labeled neurons in brainstem structures as a function of the location of the injection site along the tonotopic axis of the DCN. Our conclusion is that collaterals of VCN planar multipolar cells innervate the ipsilateral LSO. Part of this work was presented in preliminary form at the 25th annual midwinter research meeting of the Association for Research in Otolaryngology, January 27–31, 2002, St. Petersburg Beach, Florida.

MATERIALS AND METHODS

The present report is based on data obtained from eight male Sprague-Dawley rats weighing between 290 and 385 g. All animals and procedures were used in accordance with the NIH guidelines and with the approval of the Johns Hopkins Medical School Animal Care and Use Committee.

Dye injection and tissue processing

Our methods for exposing and injecting the DCN with BDA (mw 10,000; Molecular Probes, Eugene, OR) have been described in detail previously (Doucet and Ryugo, 1997) and so will be outlined only briefly. Each rat was anesthetized with an intraperitoneal injection of sodium pentobarbital (40 mg/kg) and then given an intramuscular injection of atropine sulfate (0.05 mg) to reduce mucous secretions. When the animal was areflexic to a paw pinch, the soft tissues overlying the dorsal aspect of the skull were removed, the occipital bone overlying one side of the cerebellum was drilled away, and a portion of the cerebellum was aspirated in order to view the DCN. The tip of a glass electrode (15–25 μm inner diameter) filled with a 10% solution of BDA [in 0.01 M phosphate buffer (PB), pH 7.4] was lowered 200–250 μm below the surface of the DCN. Positive current pulses (5μA; 7 seconds on, 7 seconds off) were used to inject BDA for 4–5 minutes. Subsequently, gel foam was used to fill the space created by the aspirations, the skin sutured, and the animal allowed to recover.

Animals were allowed to survive for between 3 and 13 days. The rats were then perfused with 4% paraformaldehyde in 0.12 M PB (pH 7.4). Brains were placed in a 30% sucrose solution (in 0.1 M PB, pH 7.4) for 1 or 2 days at 4°C. They were then frozen, and 50-μm coronal sections were cut through the brainstem using a sliding microtome. Every section through the CN and the SOC was saved, whereas we processed every other section through the inferior colliculus (IC). For five cases, BDA-filled structures were revealed using standard procedures (ABC Elite; Vector, Burlingame, CA) with nickel-enhanced diaminobenzidine. Sections were mounted on subbed slides and air dried overnight; then, half were stained with cresyl violet, and all were coverslipped with Permount. At this point, BDA-filled structures appear black when viewed with the light microscope. For three cases, sections were incubated overnight at 4°C in a solution of streptavidin conjugated to indocarbocyanine (Cy3; Jackson Immunoresearch Laboratories; West Grove, PA; 1:10,000 in 0.12 M PBS, pH 7.4). After washing, the sections were mounted on subbed slides and coverslipped with Krystalon (Harleco; EM Science, Gibbstown, NJ). For these three cases, BDA-filled structures appear red when viewed with a fluorescent microscope and a rhodamine barrier filter.

In seven rats, the injection sites were restricted to the DCN (see, e.g., Fig. 1A). In one rat, the injection site spilled into the dorsal acoustic stria (DAS) beneath the

DCN (see Fig. 7). For this same rat, we had cut the DAS medial to the DCN immediately after injecting BDA into the DCN.

Data analysis

In all cases, we observed retrogradely labeled cells and anterogradely labeled axons and swellings in several brainstem structures. In this report, we focus on the anterograde labeling in the LSO and describe those aspects of the data relevant to identifying the source of this label.

In seven rats, we counted retrogradely labeled cells in the VCN, the SOC, and the IC. The retrograde and anterograde labeling in the remaining rat was too sparse and light for quantitative analysis. Counts were performed using 15× eyepieces and a 40× objective (NA 0.95). The nucleolar criterion was not used, because many times the label obscured the nucleus. Labeled cells were counted in every section. The total number of labeled cells in the IC was estimated by doubling the final count. In three experiments, we did not count cells in the IC because the Cy3 signal was too weak compared with background.

For all eight cases, the pattern of retrograde and anterograde labeling in the VCN and LSO was summarized by constructing photomontages of three to five evenly spaced sections through each structure (10× objective). In three rats, the location of axonal swellings with respect to the borders of SOC nuclei was plotted in two or three evenly spaced sections through the LSO using a Nikon E600 microscope and Neurolucida hardware and software (Microbrightfield Inc., Essex, VT). The outlines of the SOC nuclei were drawn at low magnification (10× objective), and the position of the swellings was plotted at high magnification (100× objective).

All photographs were collected using a CCD color camera (Hamamatsu C5810) interfaced with a Macintosh G3 computer and imported into Adobe Photoshop (v6.0). Photomontages were constructed within Photoshop. Photomicrographs and photomontages were altered (if necessary) using procedures consistent with standard darkroom techniques.

Identifying SOC nuclei

Most subdivisions of the SOC were defined using previously published criteria (Osen et al., 1984; Faye-Lund, 1986; Vetter et al., 1991). The borders of the LSO, medial superior olive (MSO), MNTB, and superior paraolivary nucleus (SPN) are easily recognized. The borders of the surrounding periolivary nuclei are less clear. In the present study, regions caudal and rostral to the LSO are referred to as *caudal periolivary nuclei* (CPO) and *rostral periolivary nuclei* (RPO). In sections through the LSO, periolivary areas were partitioned into three regions. First, the ventral nucleus of the trapezoid body (VNTB) is located ventral to the MSO, SPN, and MNTB. VNTB neurons are heterogeneous with respect to size and shape, and they appear to be organized into rows interleaved with fascicles of trapezoid body (TB) fibers. Many VNTB cells are elliptical or oval, with the long axis oriented parallel to TB fibers. Second, the lateral nucleus of the TB (LNTB) is situated ventral to the LSO and lateral to the VNTB. The LNTB can be distinguished from the VNTB by a population of large, oval cells whose long axis is oriented parallel to the dorsoventral axis. Third, we refer to a thin shell surrounding the lateral, dorsal, and medial borders of the LSO as the *peri-LSO* (Thompson and Thompson, 1991). Regions directly ventral to the LSO are included within the LNTB.

RESULTS

Labeling in the VCN

In seven of eight rats, BDA injection sites (Fig. 1A) were restricted along the tonotopic axis of the DCN and did not spill into the underlying DAS. Collectively, the injection sites spanned most of the tonotopic axis (drawing just below Fig. 1A). In each of these seven cases, a distinctive and reliable pattern of labeling was observed in the VCN. This pattern and the VCN cell types filled by such an injection have been described in detail previously (Doucet and Ryugo, 1997; Doucet et al., 1999b) and so will only be summarized. Microneurons and axons were labeled and distributed within the granule cell domain (GCD). In the magnocellular core, the majority of the BDA labeling was confined to a thin band of filled somata, dendrites, axons, and swellings (Fig. 1B,C). This pattern was observed in most sections through the VCN. The labeled band resembles a VCN isofrequency lamina, defined as a collection of VCN neurons that are sensitive to the same range of frequencies.

Injections of BDA can produce "Golgi-like" labeling of neurons, which allows the filled cells to be classified according to their dendritic morphology. Retrogradely labeled VCN cells were classified as "multipolar" based on their multiple primary dendrites and the relatively straight trajectory of their dendrites. Bushy cells are another morphological class of VCN neurons. In contrast to multipolar cells, their dendritic morphology is characterized by one or two primary dendrites that branch profusely in a cluster near the cell body (Cant and Morest, 1979; Saldaña et al., 1987). We did not observe labeled bushy cells in these experiments, and the rostral pole of the AVCN, the home of many SBCs, is essentially devoid of labeled cells (Fig. 2).

BDA-filled multipolar cells consisted of at least three distinct groups: planar, radiate, and marginal. Members of each class exhibited a different distribution with respect to the labeled band and thus a different pattern of axonal projections to the DCN. Planar cells and their dendrites were confined primarily to the labeled band. This distribution suggests that their projections are organized tonotopically. Radiate neurons were found inside and outside the labeled band, and their dendrites extend widely across the frequency axis of the VCN. Marginal neurons were typically located within and dorsal to the labeled band in the small cell region that is squeezed between the GCD and the magnocellular core. The distribution of radiate and marginal neurons suggests that they provide both on- and off-frequency information to DCN neurons. Planar cells are more numerous than radiate or marginal cells. We counted the somata located inside the labeled band (mostly planar cells) and outside the band (mostly radiate and marginal cells). In six rats, the inside/outside ratio ranged from 2.5 to 8.6 (mean 4.8 ± 2.8).

Anterograde labeling in the SOC

In each rat, labeled axons and swellings were observed in the VCN, the SOC, nuclei of the lateral lemniscus (NLL), and the IC on both sides of the brain. In the VCN and SOC, the amount of anterograde labeling was greater

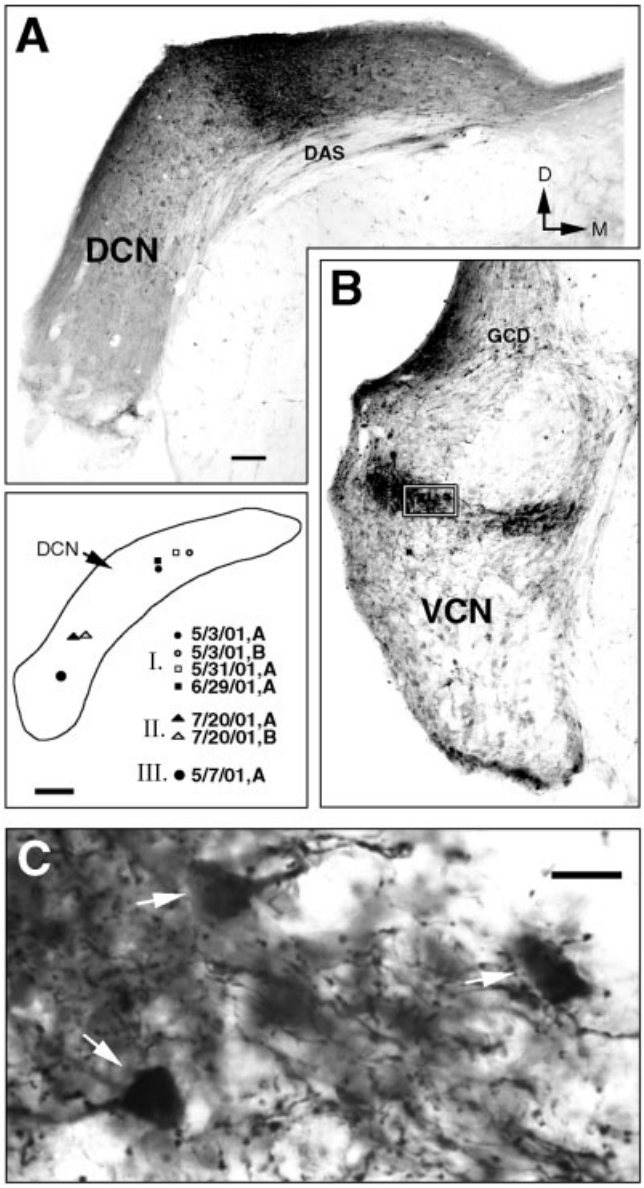

Fig. 1. Retrograde labeling in the ipsilateral VCN after an injection of BDA in the DCN. A–C display data from rat 5/3/01, A. **A:** Photomicrograph of a coronal section through the DCN illustrates a BDA injection site from a typical case. Note that the reaction product is confined to the DCN and that it is restricted along the dorsomedial/ventrolateral (tonotopic) axis. The center of the injection site for each rat is displayed beneath this panel, and the centers cluster into three groups (I, II, and III). The injection site for the eighth rat is shown in Figure 7. **B:** Photomicrograph of a coronal section through the posterior VCN. Several microneurons are labeled in the granule cell domain (GCD) dorsal to the VCN and along the lateral border of the nucleus. Note that the majority of the retrograde labeling in the VCN core is confined to a band that runs across the medial/lateral axis. Through serial sections, individual bands align and resemble a VCN isofrequency sheet. **C:** A high-magnification photomicrograph of the BDA-filled structures in the band (box in B). The band is filled with labeled cell bodies (arrows), dendrites, axons, and numerous swellings that are presumably axon terminals. Scale bar in A = 100 μm for A,B; bar in diagram = 250 μm; bar in C = 25 μm.

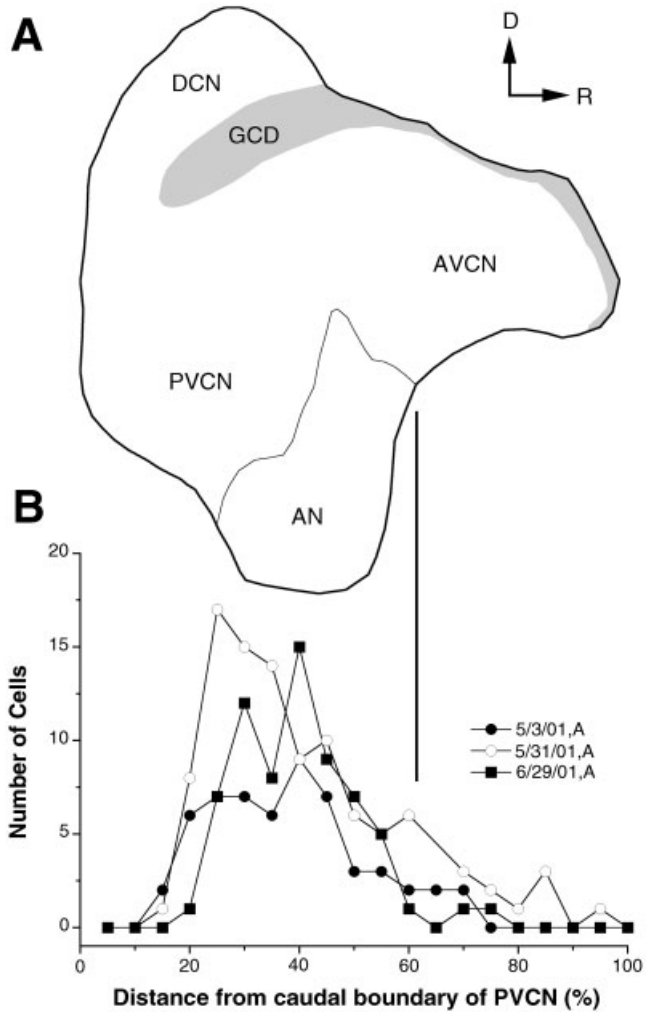

Fig. 2. Distribution of retrogradely labeled neurons within the ipsilateral VCN after an injection of BDA in the DCN. **A:** Drawing tube reconstruction of a sagittal section through the cochlear nucleus (CN) that displays the auditory nerve root (AN) and the dorsal (DCN), posteroventral (PVCN), and anteroventral (AVCN) divisions of the nucleus. **B:** Plot displaying the distribution of labeled cells for three cases. The x-axis is the distance from the caudal boundary of the PVCN normalized by the length of the VCN, and it is aligned with the drawing. Note that most of the labeled cells are located in the PVCN or near the root of the AN. The lack of filled cells in the anterior region of the AVCN is evidence that SBCs are not labeled after BDA injections in the DCN.

ipsilateral to the injection site, whereas there was more of such labeling on the contralateral side in the NLL and IC. For this report, we confined our analysis to the SOC and in particular the LSO.

Figure 3 displays the typical pattern of labeling in the SOC. Across the different cases, filled axons and swellings consistently were observed bilaterally in the CPO and RPO (data not shown). In sections through the LSO, labeling was observed ipsilaterally in the LSO and LNTB, contralaterally in the SPN, and bilaterally in the peri-LSO and VNTB. The remaining SOC nuclei contained a few filled swellings or were devoid of labeling.

The most striking feature of the labeling pattern in the SOC was a thin band of BDA-filled axons and swellings in

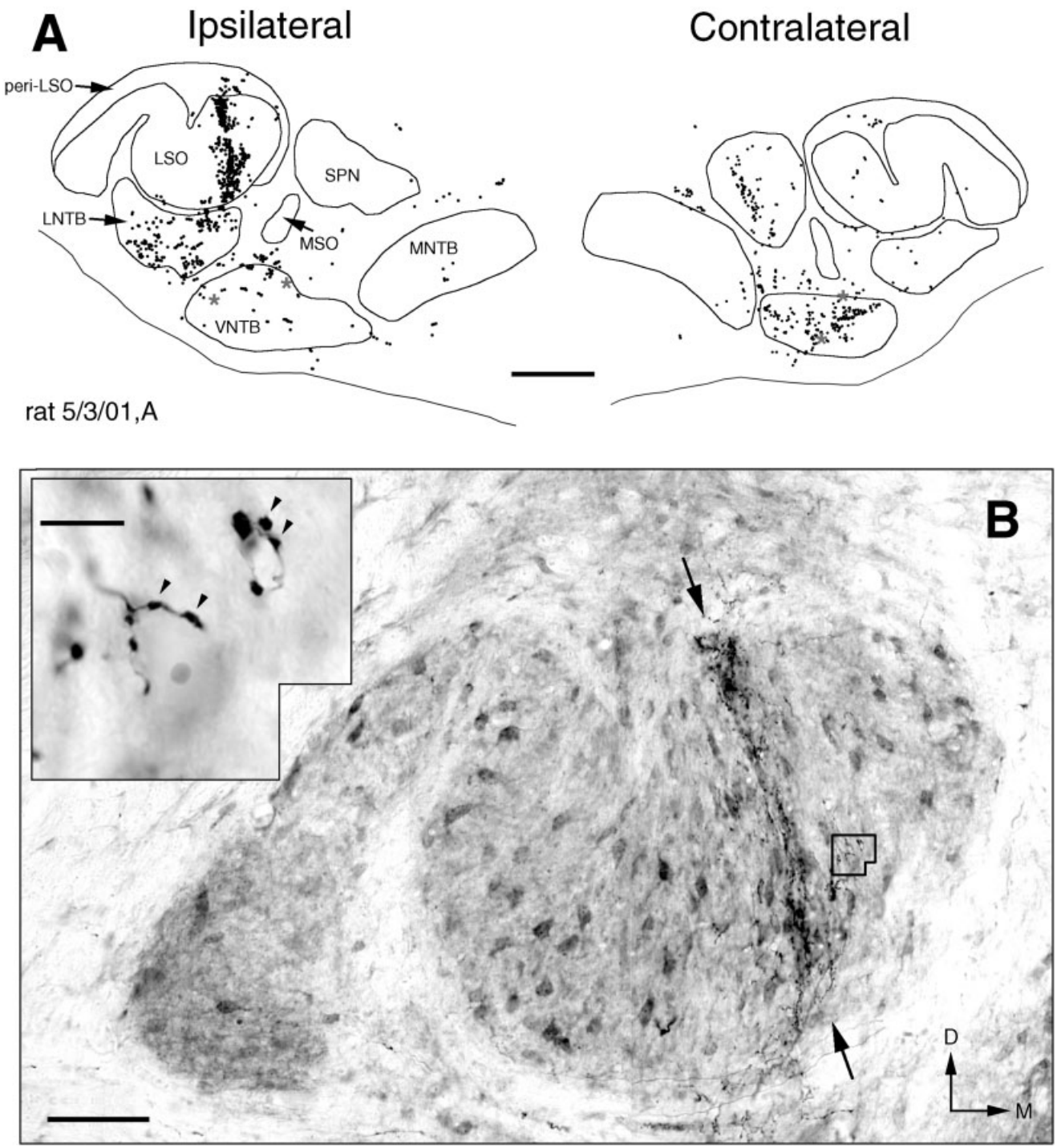

Fig. 3. Distribution of axonal swellings in the superior olivary complex (SOC) after an injection of BDA in the DCN. **A:** Low-magnification drawing of the SOC ipsilateral and contralateral to the injection site. Dots denote axonal swellings, and each asterisk signifies a retrogradely labeled cell. Note the band of swellings in the ipsilateral lateral superior olive (LSO). **B:** Photomontage of the ipsilateral LSO taken from the same coronal section drawn in A. The BDA labeling is confined to a narrow band (arrows) that contains thin axons marked by en passant and terminal swellings. The **inset** (position is denoted inside the LSO) is a high-magnification photograph of a few representative swellings. D, dorsal; LNTB, lateral nucleus of the trapezoid body; M, medial; MNTB, medial nucleus of the trapezoid body; MSO, medial superior olive; SPN, superior paraolivary nucleus; VNTB, ventral nucleus of the trapezoid body. Scale bars = 500 μm in A, 100 μm in B, 10 μm in inset.

the ipsilateral LSO (Fig. 3). Within the band, axons formed mostly en passant swellings, but terminal swellings were also observed. They were clustered around the somata of some LSO cells but more often were observed in the neuropil (inset, Fig. 3B). The labeled band was observed throughout the length of the LSO (Fig. 4). LSO principal cells are shaped like discs, with dendrites flattened in the medial-lateral dimension and elongated in the rostral-caudal dimension (Scheibel and Scheibel, 1974). Principal cells and their dendrites align with incoming axons (Ramón y Cajal, 1909; Scheibel and Scheibel, 1974; Sanes et al., 1990) and form fibrodendritic layers that are thought to be the anatomical substrate for isofrequency laminae. In our experiments, when adjacent sections through the LSO are aligned as in Figure 4, the band of labeling creates a three-dimensional sheet resembling an isofrequency lamina.

The labeling in the ipsilateral LNTB, LSO, and peri-LSO appeared to arise from thin collaterals that sprouted from thicker axons in the TB (Fig. 5A). The collaterals exhibited a ventrolateral to dorsomedial trajectory and together formed a stripe of labeling through these three SOC nuclei (see, e.g., Fig. 4B). It was impossible to trace every individual collateral from its branch point into the LSO, because there were simply too many labeled fibers and the distance traversed was too great. Nevertheless, we observed a few collaterals in each rat that could be followed along their route into the LNTB and LSO, where they formed axonal swellings.

One source of labeled axons in the TB is BDA-filled multipolar cells in the VCN. We observed axons near the medial border of the labeled band in the VCN that could be followed into the TB (Fig. 5B). At the border of the VCN, some labeled axons gave rise to thin, dorsally running collaterals (Fig. 5C). The position and orientation of these collaterals make them strong candidates for the ventrotubercular projection to the DCN. We were unable to determine whether the parent axons producing putative ventrotubercular collaterals (Fig. 5C) were the same as those producing SOC collaterals (Fig. 5A).

A second prominent bundle of labeled fibers was observed in the DAS medial to the injection site. A major source of these axons was undoubtedly filled DCN pyramidal and giant cells. These axons terminate in the contralateral IC (data not shown), as reported previously (Osen, 1972; Strominger, 1973). For one rat, we severed the axons of pyramidal and giant cells by cutting the DAS after injecting BDA into the DCN. We wanted to determine whether DCN neurons contributed to the anterograde labeling in the ipsilateral LSO. The result was that axonal labeling in the contralateral IC was virtually eliminated, whereas large numbers of axons and swellings were still observed in the LSO (see Fig. 7). Thus we confirmed that DCN neurons do not project to the ipsilateral LSO (Osen, 1972; Warr 1982).

Topography of projections to the LSO

A topographic relationship was observed among the locations of the DCN injection site, the labeled band in the ipsilateral VCN, and the band of filled axons and swellings in the ipsilateral LSO. The locations of the DCN injection sites clustered into three groups (Fig. 1). With respect to the issue of topography, results among members of the same group were indistinguishable. Therefore, Figure 6 displays data from three cases, one from each group. All three nuclei are organized tonotopically (DCN: Ryan et al., 1988; Kaltenbach and Lazor, 1991; Spirou et al., 1993; VCN: Clopton et al., 1974; Bourk et al., 1981; LSO: Tsuchitani and Boudreau, 1967; Guinan et al., 1972; Friauf, 1992), and the position of cells tuned to high frequencies and those most sensitive to low frequencies is indicated in the middle row. As the injection site shifts from high- to low-frequency regions of the DCN (top to bottom row), there is an orderly shift of the labeled bands in the VCN and LSO from higher to lower frequency regions of these nuclei. Recall that the labeled band in the VCN contains planar multipolar cells (Fig. 1). The data in Figure 6 are thus consistent with the hypothesis that planar cells are a source of the labeled axons and swellings in the LSO.

If the injection site and labeled bands are located in corresponding frequency regions of each nucleus, then the data in Figure 6 suggest that the spatial representation of frequency differs across these structures. For example, an injection site clearly located in the lateral half of the DCN (middle row, Fig. 6) results in a band of labeling that nearly bisects the VCN and LSO. When the injection site is located even more laterally in the DCN (bottom row, Fig. 6), the labeled band in the VCN shifts toward the ventral border, but the band in the LSO does not invade the lateral limb. In fact, we did not observe labeled axonal swellings in the lateral (low frequency) limb of the LSO.

Retrograde labeling in the brainstem

In principle, all structures that contain labeled neurons could be a source of collateral fibers in the LSO. The VCN is one such structure, but BDA-filled somata were observed bilaterally in several brainstem nuclei. In the ipsilateral VCN, the BDA reaction product was distributed uniformly throughout the soma and frequently filled the entire dendritic tree of the cells. This type of labeling was also observed in the SOC, but, for many SOC cells, the reaction product appeared granular and was often confined to the soma. We counted the labeled cells regardless of the darkness of staining and display the results in Table 1.

For most nuclei, the number of labeled neurons was small and/or highly variable. Typically, there was at least one case in which the number of filled cells was under 10. In contrast, the amount of labeling in the LSO was robust in all rats. Structures that were sparsely and variably marked with filled cells are almost certainly not major contributors to the labeling in the LSO. IC neurons can be eliminated as a source, because they do not project to the LSO (Faye-Lund, 1986; Caicedo and Herbert, 1993; Malmierca et al., 1996).

The ipsilateral VCN and the contralateral VNTB consistently contained a large number of retrogradely labeled cells. In addition, the location of labeled cells in the contralateral VNTB appeared to be related topographically to the position of the DCN injection site (data not shown). However, several observations favor the idea that VCN neurons are responsible for the majority of the labeling in the LSO. First, labeling in the VCN reliably revealed darkly stained somata and dendrites, whereas such labeling in the VNTB was many times light, granular, and confined to the cell body. Second, the average number of filled neurons in the VCN was four times that in the contralateral VNTB. Third, the amount of labeling in the LSO appeared to be quite stable across rats. The number of labeled cells in the VCN was also quite stable [standard deviation (SD) = 24% of the mean] when compared with

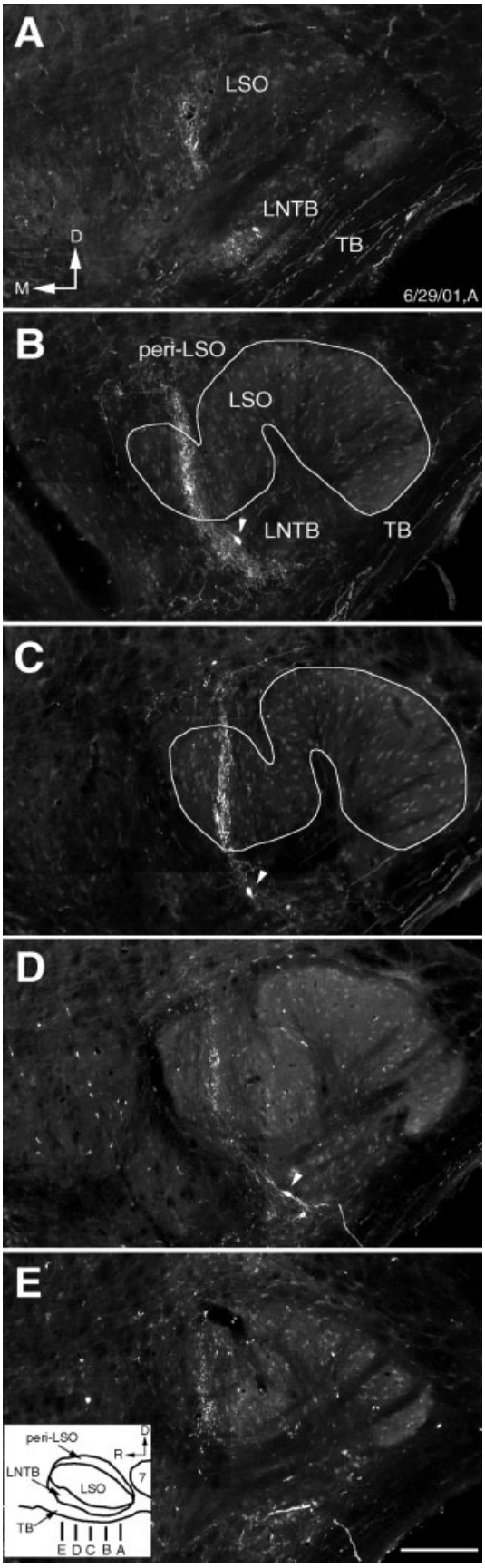

that seen in the VNTB (SD = 44% of the mean). Finally, in one case, the BDA injection spilled into the DAS (Fig. 7A), and the number of retrogradely labeled cells in the ipsilateral VCN was nearly twice the average seen in the other rats (Fig. 7B, Table 1). In contrast, the number of labeled cells in the contralateral VNTB was near the average. In this case, we observed a dramatic increase in the amount of anterograde labeling in the ipsilateral LSO (Fig. 7C). Furthermore, the spread of the labeled axons and swellings over the medial limb of the LSO is what one would expect if VCN multipolar cells were the primary source of this labeling (Fig. 7D).

DISCUSSION

Our main conclusion is that planar multipolar cells of the VCN give rise to a topographically organized projection to the ipsilateral DCN and LSO (Fig. 8). This conclusion is based on light microscopic analyses of results obtained from discrete BDA injections in the DCN of rats that produced a narrow band of labeled axons and swellings in the ipsilateral LSO. We assume that the axonal swellings represent presynaptic terminals. Within the VCN, BDA-filled multipolar cells fall into at least three groups: planar, radiate, and marginal. Radiate neurons project to the DCN and the contralateral CN (Doucet et al., 1999a). The axons of these cells exit the CN by way of the DAS (Cant and Gaston, 1982; Schofield and Cant, 1996; Doucet and Ryugo, unpublished observations); therefore, they cannot be responsible for the labeled collaterals in the TB that innervate the LSO (Fig. 5). In each experiment, between five and fifteen marginal neurons were sprinkled across the tonotopic axis of the VCN. The modest number of labeled marginal cells and their apparent nontopographic organization minimize their potential as a source for the pathway to the LSO. In contrast, large numbers of labeled planar cells were observed in each rat, and there is a reliable topographic relationship between their location in the VCN and the band of labeling in the LSO. Consequently, we propose that most of the filled axons in the LSO represent the collaterals of planar cells.

We cannot rule out the possibility that, in some cases, retrogradely labeled cells in the ipsilateral LNTB and/or the contralateral VNTB also contributed to the labeling in the LSO. Prior studies that injected horseradish peroxidase into the LSO showed very few retrogradely labeled cells in these two SOC nuclei, suggesting only a weak connection (Glendenning et al., 1985; Cant and Casseday,

Fig. 4. Photomontages of five fluorescent coronal sections (**A–E**) through the LSO ipsilateral to the injection site. For this rat, we injected the right DCN and visualized BDA-filled structures with streptavidin-Cy3 (labeled structures appear white). In the **inset**, the position of the sections along the rostral/caudal axis of the LSO is shown. The distance between sections is approximately 150 μm. Note that in each section the majority of the LSO label is confined to a thin band. All five sections are aligned with respect to the medial/lateral axis, and the bands are "in register" with each other. In three dimensions, the labeled bands form a continuous sheet that runs rostral-caudally through the nucleus and resembles an LSO isofrequency lamina. In some sections (see, e.g., B and C), the band of labeled axons, swellings, and neurons (some denoted by arrowheads) clearly extend beyond the LSO and into the LNTB and peri-LSO. TB, trapezoid body; 7, facial nucleus. Scale bar = 200 μm.

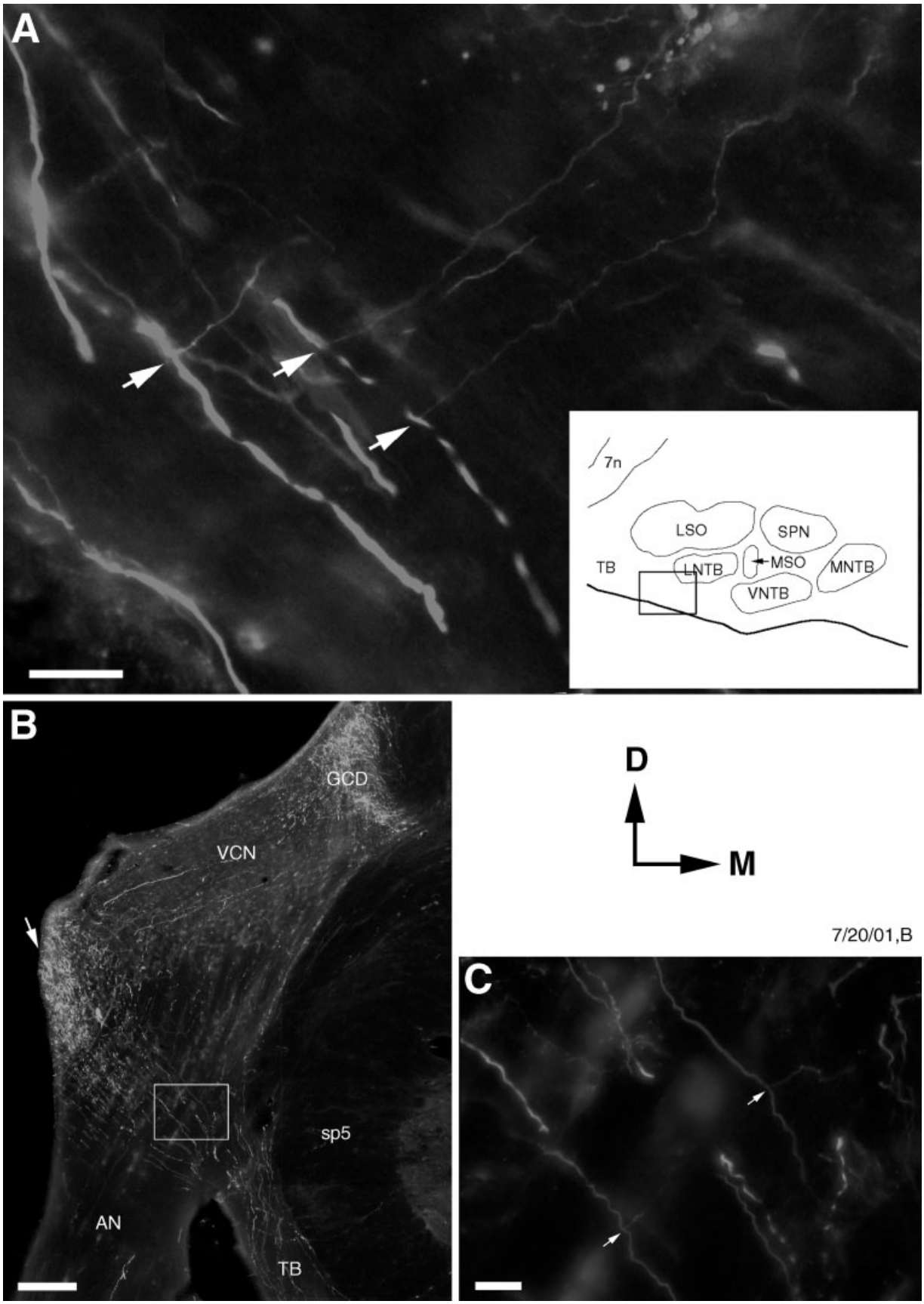

Fig. 5. BDA-filled axons and collaterals within the VCN and TB labeled with fluorescent streptavidin-Cy3. **A:** High-magnification photomontage of labeled TB axons with collateral branches. The **inset** displays the location of these collaterals ventral to the LNTB and LSO. Thin collaterals (arrows) branch from thicker axons and some can be followed into the LNTB, where they form terminal swellings. **B:** Photomontage of a coronal section through the VCN and the AN. The majority of the labeling is confined to the GCD and a band (arrow) near the ventral border of the VCN. Several filled axons are located medial to the band and can be followed into the TB. These fibers are inferred to arise from labeled planar multipolar cells within the band (see text). One or two darkly labeled fibers in the AN are probably retrogradely labeled AN fibers that innervate the DCN injection site. **C:** High-magnification photomicrograph of the region denoted by the box in B. Thin collaterals (arrows) project dorsally toward the DCN and may represent ventrotubercular axons. sp5, Spinal trigeminal tract; 7n, seventh (facial) nerve (see also legend to Fig. 3). Scale bars = 25 μm in A,C, 200 μm in B.

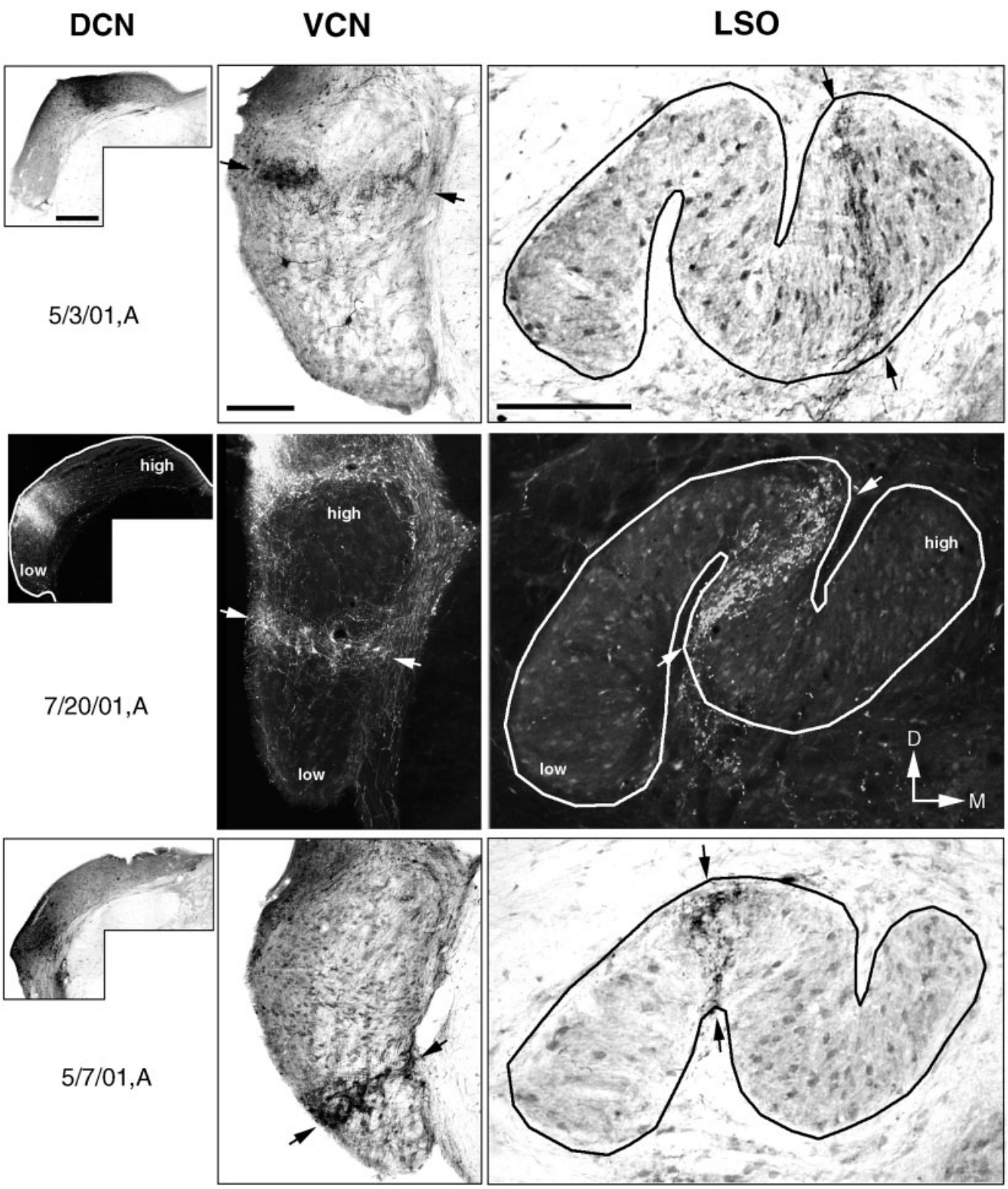

Fig. 6. Photomontages illustrating the topographic relationship between the injection site in the DCN and BDA-filled structures in the ipsilateral VCN and LSO. Data from separate rats are displayed in each row. For the middle row, we labeled the general location of cells in each structure tuned to high frequencies and those tuned to low frequencies. The position of the coronal section along the rostral-caudal axis of each structure is approximately the same. In the left column, note that the location of each injection site shifts to progressively lower frequency regions of the DCN. The position of the labeled band in the VCN and the LSO (arrows in each column) shifts accordingly. This topographic relationship is consistent with the idea that VCN planar cells located in the labeled band are a source of the filled axons and terminals in the LSO. Scale bars = 250μm and apply to figures in the same column.

TABLE 1. Number of Retrogradely Labeled Neurons in Brainstem and Midbrain Auditory Nuclei Following an Injection of BDA Into the Dorsal Cochlear Nucleus

	Retrograde labeling in															
	Ipsilateral									Contralateral						
Cases	VCN	LSO	Peri-LSO	LNTB	VNTB	CPO	RPO	Other	IC	LSO	Peri-LSO	LNTB	VNTB	CPO	RPO	IC
5/3/01,A	200	13	5	29	19	2	14	0	18	1	4	2	54	3	0	7
5/7/01,A	156	5	11	8	13	0	3	0	27	0	1	0	35	0	8	18
5/31/01,A	284	9	13	33	16	3	27	0	74	0	4	4	40	2	17	45
6/29/01,A	164	4	10	25	2	0	3	1	—	0	2	1	60	2	9	—
7/20/01,A	207	3	12	10	4	1	12	2	—	0	4	0	93	0	6	—
7/20/01,B	251	2	19	20	17	1	2	0	—	0	1	1	32	0	5	—
Average	210	6	12	21	12	1	10	1	40	0	3	1	52	1	8	23
5/31/01,B[1]	448	4	4	12	32	8	13	8	70	0	2	0	54	2	18	32

[1]BDA injection spread into the DAS, and the DAS was cut medial to DCN. Data from this animal are not included in the averages. See Materials and Methods for the definition of SOC nuclei.

1986). However, the axons of individual LNTB neurons filled in a slice preparation can be traced into the ipsilateral LSO (Kuwabara and Zook, 1992). Injections of BDA into the VNTB can produce terminal labeling in the contralateral LSO (Warr and Beck, 1996). These recent studies indicate that more work is needed to resolve the extent to which the LNTB and VNTB represent sources of input to the LSO. Still, in this paper, we argue that VNTB and LNTB neurons represent only a *minor* source of labeling in the LSO for reasons that have already been delineated (see Results).

The conclusion that planar cells project to the LSO is consistent with the findings of prior investigators. For example, lesions within the globular bushy and multipolar cell area in cats resulted in axonal degeneration in the ipsilateral LSO (Warr, 1982). Injection of retrograde tracers into the LSO of the cat labeled cells in the PVCN, where multipolar cells are the dominant cell type. However, the cells could not be classified based on their dendritic morphology, because the tracers did not fill the dendrites (Glendenning et al., 1985; Cant and Casseday, 1986). Direct injections of anterograde tracers into the PVCN of cats and guinea pigs revealed a topographically organized projection to the ipsilateral LSO, but the injection site obscured the cell types that sent the axons (Thompson and Thompson, 1987, 1991; Thompson, 1998). Finally, single-cell-labeling studies in the cat and rat VCN have provided a few but nonetheless unambiguous instances in which axons of multipolar cells are traced into the ipsilateral LSO (Rouiller and Ryugo, 1984; Friauf and Ostwald, 1988). In the present report, BDA produced "Golgi-like" filling of VCN neurons, allowing the classification of planar cells to be based on dendritic morphology as well as projection pattern. Thus our results confirm earlier reports that VCN multipolar cells, in addition to SBCs, innervate the ipsilateral LSO and extend these findings by identifying the planar cell type as a source of this input.

Technical considerations and labeling outside the LSO

Planar cell projections to the DCN and the properties of BDA can account for the observed labeling patterns (see, e.g., Fig. 7D). BDA has two features that are relevant to this discussion. First, neurons filled with BDA transport the dye both anterogradely and retrogradely (Veenman et al., 1992; Rajakumar et al., 1993; Reiner et al., 2000). Second, collateral–collateral transport of BDA within single cells is quite effective in central neurons (Chen and Aston-Jones, 1998). As a result, BDA can fill the entire axon of a cell with injection into the terminal field of a single collateral. When BDA is injected into the terminal fields of planar cell collaterals in the DCN, they transport the tracer retrogradely to fill their somata and dendrites in the VCN. Additionally, BDA is transported anterogradely by the parent axon into the TB and fills collateral axons that target the ipsilateral LSO. When the injection site is shifted to different frequency regions of the DCN, the set of labeled planar cells shifts to the corresponding frequency regions in the VCN, as do their labeled collaterals in the LSO (see Fig. 8). When BDA spills into the DAS, planar cells that project into the injection site will be filled as well as those targeting higher frequency regions because of the labeling of "axons of passage" (Fig. 7D).

The pattern of terminal labeling in the SOC described here is similar to that described when the PVCN—home to most planar cells (Fig. 2)—was injected with an anterograde tracer (Thompson and Thompson, 1991). This correspondence suggests that planar cells might be responsible for most of the labeled terminals that we observed in the SOC. In some coronal sections, the collaterals in the TB that targeted the LSO formed a bundle that also innervated the LNTB and the peri-LSO (see, e.g., Fig. 4B). We are confident that planar cells are also responsible for most of the labeling in these two regions. The location of terminals in the peri-LSO was related topographically to the DCN injection site (summarized in Fig. 8), whereas that in the LNTB was more diffuse (see, e.g., Fig. 3). For terminals in other regions of the SOC, such as the VNTB or contralateral LSO, several factors prevent us from assigning a source. First, there were fewer terminals in these areas, and their topographic relationship with the injection site, if one exists, was more complicated. Second, we could not trace the axonal source of these terminals to a particular neuron or fiber tract. Third, given the properties of BDA described above and how little is known about the local projections of SOC cells, we cannot exclude the retrogradely labeled SOC neurons as sources for the labeled terminals.

Functional considerations

LSO principal cells are sensitive to intensity differences between the two ears (Tsuchitani and Boudreau, 1966, 1967; Goldberg and Brown, 1969). They respond to small

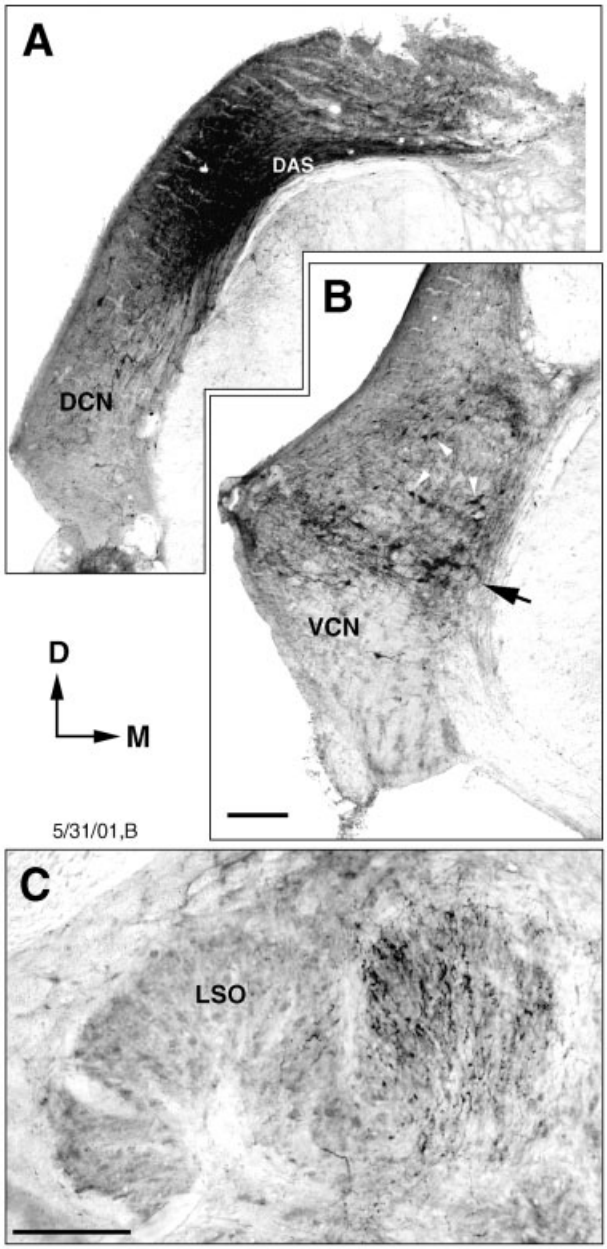

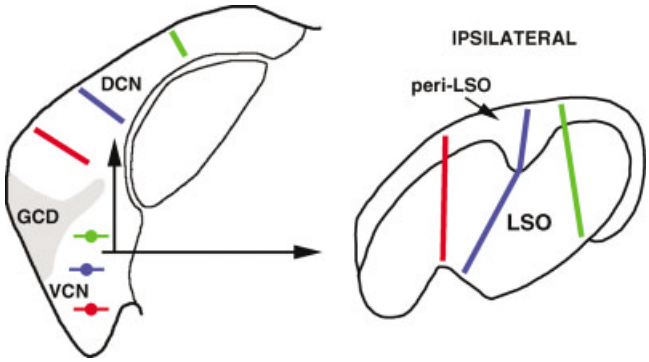

Fig. 8. Diagram summarizing our conclusions. Three VCN planar cells are drawn in three different isofrequency laminae: high (green), middle (blue), and low (red). The terminal field of each planar cell in the ipsilateral DCN, LSO, and peri-LSO is illustrated with corresponding colors. Our conclusion is that VCN planar cells project collateral axons to the DCN and LSO. The labeling patterns suggest that these projections are tonotopically organized. Planar cell axons also cross the midline and target cells in the contralateral inferior colliculus (not shown). See earlier figure legends for abbreviations.

intensity differences even when the average level of the sound in each ear is quite high (Boudreau and Tsuchitani, 1968; Tollin and Yin, 2002a). These features imply that the LSO receives input from CN pathways that encode intensity. Our finding that planar cells, in addition to SBCs, project to the LSO prompts us to consider how these two pathways might contribute to the coding of intensity.

SBCs correlate with the physiological unit type referred to as *primary-like* units; they respond to sound in a fashion that resembles that of auditory nerve fibers (Rhode et al., 1983; Rouiller and Ryugo, 1984). Primary-like units are thought to preserve the pattern of activity in the auditory nerve and relay this temporal information to their targets in the brainstem (Molnar and Pfeiffer, 1968; Rhode and Smith, 1986; Young et al., 1988). This idea is supported by the projections of SBCs to the MSO, a nucleus containing cells that are sensitive to timing differences between the two ears (Goldberg and Brown, 1969; Yin and Chan, 1990). The role of SBC input to the LSO is less clear. Historically, stimulus intensity was thought to be encoded by the firing rate of auditory nerve fibers and

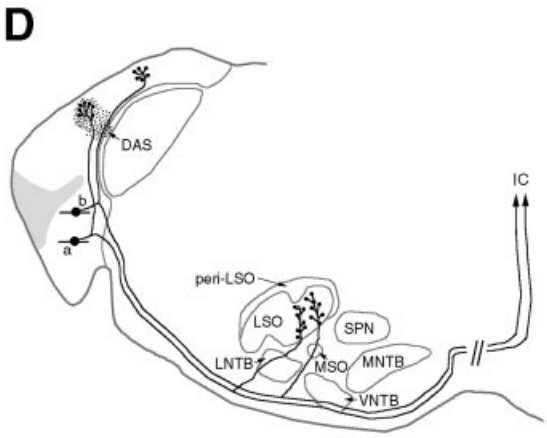

Fig. 7. Labeling in the ipsilateral VCN and LSO after a BDA injection that encroached on the DAS. **A:** Photomontage of a coronal section through the DCN displaying the BDA injection site. Note that the center of the injection site is deeper than for the case shown in Figure 1. The injection spilled into the DAS. **B:** Photomontage of coronal section through the VCN. A band of labeling (arrow) is observed, but there are also many labeled cells dorsal to the band (a few denoted with arrowheads). **C:** Photomontage of coronal section through the LSO. Note that labeled axons and swellings are located throughout much of the medial limb of the LSO. **D:** Drawing displaying our interpretation of the labeling patterns in the VCN and LSO observed for this case. The injection (stippled region) labels VCN neurons that project to the center of the injection site (cell a) and also neurons sensitive to higher frequencies via fibers-of-passage (cell b). For this case, if VCN neurons are a significant source of the axonal labeling in the LSO, one would predict an expansion of the LSO label within the medial (high-frequency) limb of the LSO as shown. A and B are presented at identical magnifications. Scale bars = 200μm.

not the precise times at which they fire (see Viemeister, 1988; Delgutte, 1996). Recent modeling studies, however, suggest that intensity may be encoded in the temporal pattern of activity in the nerve (Carney, 1994; Heinz et al., 2001). Furthermore, GBCs, another CN cell type implicated in processing temporal information (Joris et al., 1994a,b), appear to be the sole origin of the pathway from the opposite ear to the LSO. Thus the activity of bushy cells may convey intensity information to the LSO via their sensitivity to temporal patterns in the auditory nerve.

Planar cells belong to the morphological class refered to as *multipolar* or *stellate* neurons. These cells correlate with the physiological type named *chopper* or *onset* units (Rhode et al., 1983; Rouiller and Ryugo, 1984). We have argued previously that planar cells are most likely "chopper" units (see Doucet and Ryugo, 1997). Chopper units have been hypothesized for many reasons to encode intensity. For example, their intrinsic membrane properties (Oertel et al., 1988) combined with the distribution of inputs on their soma and dendrites (Cant, 1981) seem to sensitize them to the firing rate of auditory nerve fibers (Young et al., 1988). Some chopper units respond over wide ranges of intensity (Rhode and Smith, 1986) even in the presence of intense background noise (May and Sachs, 1992; May et al., 1997). It seems relevant to note that birds use IIDs to detect the elevation of a sound in space and that the neural pathways subserving IID detection are composed primarily of chopper units (Sullivan and Konishi, 1984; Takahashi et al., 1984; Mogdans and Knudsen, 1994). Our finding that planar cells project to the LSO suggests that birds and mammals share common mechanisms for encoding intensity and detecting IIDs.

Two different cell types (SBCs and planar cells) could project to the same target, or they could each synapse on different types of LSO neurons. The LSO is heterogeneous in its neuronal composition (Helfert and Schwartz, 1986, 1987; Rietzel and Friauf, 1998). Principal cells represent 75% of the population, exhibit dendrites that form a discoid and uniplanar domain, and are organized into rostral-caudal sheets oriented perpendicular to the curvature of the nucleus (Scheibel and Scheibel, 1974; Cant, 1984; Helfert and Schwartz, 1986; Majorossy and Kiss, 1990). Roughly half of these cells project to the ipsilateral IC, whereas the other half project to the contralateral IC (Glendenning and Masterton, 1983; Saint Marie et al., 1989; Brunso-Bechtold et al., 1994). The ipsilaterally projecting neurons have a high-affinity uptake system for glycine (Saint Marie and Baker, 1990) and are covered with endings containing round synaptic vesicles (Brunso-Bechtold et al., 1994). The implication is that excitatory inputs from the ipsilateral CN impinge on inhibitory LSO neurons that have an ipsilateral projection to the IC. There is also the "lateral efferent" system that in rats originates in and around the LSO (White and Warr, 1983; Aschoff and Ostwald, 1988; Warr et al., 1997). Little is known about the inputs to these lateral efferent neurons. Finally, even when labeled planar cells seem to be located in the ventral (low-frequency) region of the VCN, there is a curious lack of labeling in the lateral (low-frequency) limb of the LSO (Fig. 6). Does this pattern indicate that different frequency regions of the LSO receive different proportions of planar cell and SBC input? It seems clear that identifying the LSO targets of planar cells and SBCs will provide new insights into the structurally and functionally distinct pathways emanating from the CN and LSO.

ACKNOWLEDGMENTS

The authors are grateful for the excellent technical assistance provided by Tan Pongstaporn, Liana Rose, and Alison Wright.

LITERATURE CITED

Aschoff A, Ostwald J. 1988. Distribution of cochlear efferents and olivocollicular neurons in the brainstem of rat and guinea pig. A double labeling study with fluorescent tracers. Exp Brain Res 71:241–251.

Beyerl BD. 1978. Afferent projections to the central nucleus of the inferior colliculus in the rat. Brain Res 145:209–223.

Boudreau JC, Tsuchitani C. 1968. Binaural interaction in the cat superior olive S segment. J Neurophysiol 31:442–454.

Bourk TR, Mielcarz JP, Norris BE. 1981. Tonotopic organization of the anteroventral cochlear nucleus of the cat. Hear Res 4:215–241.

Brunso-Bechtold JK, Linville MC, Henkel CK. 1994. Terminal types on ipsilaterally and contralaterally projecting lateral superior olive cells. Hear Res 77:99–104.

Caicedo A, Herbert H. 1993. Topography of descending projections from the inferior colliculus to auditory brainstem nuclei in the rat. J Comp Neurol 328:377–392.

Caird D, Klinke R. 1983. Processing of binaural stimuli by cat superior olivary complex neurons. Exp Brain Res 52:385–399.

Cant NB. 1981. The fine structure of two types of stellate cells in the anterior division of the anteroventral cochlear nucleus of the cat. Neuroscience 6:2643–2655.

Cant NB. 1984. The fine structure of the lateral superior olivary nucleus of the cat. J Comp Neurol 227:63–77.

Cant NB. 1992. The cochlear nucleus: neuronal types and their synaptic organization. In: Webster DB, Popper AN, Fay RR, editors. The mammalian auditory pathway: neuroanatomy. New York: Springer-Verlag. p 66–116.

Cant NB, Casseday JH. 1986. Projections from the anteroventral cochlear nucleus to the lateral and medial superior olivary nuclei. J Comp Neurol 247:457–476.

Cant NB, Gaston KC. 1982. Pathways connecting the right and left cochlear nuclei. J Comp Neurol 212:313–326.

Cant NB, Morest DK. 1979. Organization of the neurons in the anterior division of the anteroventral cochlear nucleus of the cat. Light-microscopic observations. Neuroscience 4:1909–1923.

Carney LH. 1994. Spatiotemporal encoding of sound level: models for normal encoding and recruitment of loudness. Hear Res 76:31–44.

Chen S, Aston-Jones G. 1998. Axonal collateral-collateral transport of tract tracers in brain neurons: false anterograde labelling and useful tool. Neuroscience 82:1151–1163.

Clopton BM, Winfield JA, Flammino FJ. 1974. Tonotopic organization: review and analysis. Brain Res 76:1–20.

Delgutte B. 1996. Physiological models for basic auditory percepts. In: Hawkins HL, McMullen TA, Popper AN, editors. Auditory computation. New York: Springer-Verlag. p 157–220.

Doucet JR, Ryugo DK. 1997. Projections from the ventral cochlear nucleus to the dorsal cochlear nucleus in rats. J Comp Neurol 385:245–264.

Doucet JR, Cahill HB, Ohlrogge M, Ryugo DK. 1999a. Ventral cochlear nucleus multipolar neurons that innervate the dorsal cochlear nucleus differ in their projections outside the cochlear nucleus. ARO Abstr 22:148.

Doucet JR, Ross AT, Gillespie MB, Ryugo DK. 1999b. Glycine immunoreactivity of multipolar neurons in the ventral cochlear nucleus which project to the dorsal cochlear nucleus. J Comp Neurol 408:515–531.

Faye-Lund H. 1986. Projection from the inferior colliculus to the superior olivary complex in the albino rat. Anat Embryol 175:35–52.

Friauf E. 1992. Tonotopic order in the adult and developing auditory system of the rat as shown by c-fos immunocytochemistry. Eur J Neurosci 4:798–812.

Friauf E, Ostwald J. 1988. Divergent projections of physiologically characterized rat ventral cochlear nucleus neurons as shown by intraaxonal injection of horseradish peroxidase. Exp Brain Res 73:263–284.

Glendenning KK, Masterton RB. 1983. Acoustic chiasm: efferent projections of the lateral superior olive. J Neurosci 3:1521–1537.

Glendenning KK, Brunso-Bechtold JK, Thompson GC, Masterton RB. 1981. Ascending auditory afferents to the nuclei of the lateral lemniscus. J Comp Neurol 197:673–703.

Glendenning KK, Hutson KA, Nudo RJ, Masterton RB. 1985. Acoustic chiasm II: anatomical basis of binaurality in lateral superior olive of cat. J Comp Neurol 232:261–285.

Goldberg JM, Brown P. 1969. Responses of binaural neurons of dog superior olivary complex to dichotic tonal stimuli: some physiological mechanisms of sound localization. J Neurophysiol 32:613–636.

Guinan JJJ, Norris BE, Guinan SS. 1972. Single auditory units in the superior olivary complex. II: locations of unit categories and tonotopic organization. Int J Neurosci 4:147–166.

Heinz MG, Colburn HS, Carney LH. 2001. Rate and timing cues associated with the cochlear amplifier: level discrimination based on monaural cross-frequency coincidence detection. J Acoust Soc Am 110:2065–2084.

Helfert RH, Schwartz IR. 1986. Morphological evidence for the existence of multiple neuronal classes in the cat lateral superior olivary nucleus. J Comp Neurol 244:533–549.

Helfert RH, Schwartz IR. 1987. Morphological features of five neuronal classes in the gerbil lateral superior olive. Am J Anat 179:55–69.

Henkel CK, Gabriele ML. 1999. Organization of the disynaptic pathway from the anteroventral cochlear nucleus to the lateral superior olivary nucleus in the ferret. Anat Embryol 199:149–160.

Irvine DRF. 1992. Physiology of the auditory brainstem. In: Webster DB, Popper AN, Fay RR, editors. The mammalian auditory pathway: neurophysiology. New York: Springer-Verlag. p 153–231.

Irvine DRF, Park VN, McCormick L. 2001. Mechanisms underlying the sensitivity of neurons in the lateral superior olive to interaural intensity differences. J Neurophysiol 86:2647–2666.

Joris PX, Carney LH, Smith PH, Yin TC. 1994a. Enhancement of neural synchronization in the anteroventral cochlear nucleus. I. Responses to tones at the characteristic frequency. J Neurophysiol 71:1022–1036.

Joris PX, Smith PH, Yin TC. 1994b. Enhancement of neural synchronization in the anteroventral cochlear nucleus. II. Responses in the tuning curve tail. J Neurophysiol 71:1037–1051.

Kaltenbach JA, Lazor JA. 1991. Tonotopic maps obtained from the surface of the dorsal cochlear nucleus of the hamster and rat. Hear Res 51: 149–160.

Kelly JB, Liscum A, van Adel B, Ito M. 1998. Projections from the superior olive and lateral lemniscus to tonotopic regions of the rat's inferior colliculus. Hear Res 116:43–54.

Kuwabara N, Zook JM. 1991. Classification of the principal cells of the medial nucleus of the trapezoid body. J Comp Neurol 314:707–720.

Kuwabara N, Zook JM. 1992. Projections to the medial superior olive from the medial and lateral nuclei of the trapezoid body in rodents and bats. J Comp Neurol 324:522–538.

Majorossy K, Kiss A. 1990. Types of neurons and synaptic relations in the lateral superior olive of the cat: normal structure and experimental observations. Acta Morphol Hung 38:207–215.

Malmierca MS, Lebeau FEN, Rees A. 1996. The topographical organization of descending projections from the central nucleus of the inferior colliculus in guinea pig. Hear Res 93:167–180.

May BJ, Sachs MB. 1992. Dynamic range of neural rate responses in the ventral cochlear nucleus of awake cats. J Neurophysiol 68:1589–1602.

May BJ, Le Prell GS, Heinz RD, Sachs M. 1997. Speech representation in the auditory nerve and ventral cochlear nucleus. In: Syka J, editor. Acoustic signal processing in the central auditory system. New York: Plenum Press. p 413–430

Mogdans J, Knudsen EI. 1994. Representation of interaural level difference in the VLVp, the first site of binaural comparison in the barn owl's auditory system. Hear Res 74:148–164.

Molnar CE, Pfeiffer RR. 1968. Interpretation of spontaneous spike discharge patterns of neurons in the cochlear nucleus. Proc IEEE 56:993–1004.

Oertel D, Wu SH, Hirsch JA. 1988. Electrical characteristics of cells and neuronal circuitry in the cochlear nuclei studied with intracellular recordings from brain slices. In: Edelman GM, Gall WE, Cowan WM, editors. Auditory function: neurobiological basis of hearing. New York: Wiley. p 313–336.

Osen KK. 1970. Afferent and efferent connections of three well-defined cell types of the cat cochlear nucleus. In: Anderson P, Jansen JKS, editors. Excitatory synaptic mechanisms. Oslo: Universitetsforlaget. p 295–300.

Osen KK. 1972. Projection of the cochlear nuclei on the inferior colliculus in the cat. J Comp Neurol 144:355–372.

Osen KK, Mugnaini E, Dahl AL, Christiansen AH. 1984. Histochemical localization of acetylcholinesterase in the cochlear and superior olivary nuclei. A reappraisal with emphasis on the cochlear granule cell system. Arch Ital Biol 122:169–212.

Park TJ, Monsivais P, Pollak GD. 1997. Processing of interaural intensity differences in the LSO: role of interaural threshold differences. J Neurophysiol 77:2863–2878.

Rajakumar N, Elisevich K, Flumerfelt BA. 1993. Biotinylated dextran: a versatile anterograde and retrograde neuronal tracer. Brain Res 607: 47–53.

Ramón y Cajal R. 1909. Histologie du système nerveux de l'homme et des vertébrés. Madrid: Instituto Ramón y Cajal.

Reiner A, Veenman CL, Medina L, Jiao Y, Del Mar N, Honig MG. 2000. Pathway tracing using biotinylated dextran amines. J Neurosci Methods 103:23–37.

Rhode WS, Smith PH. 1986. Encoding timing and intensity in the ventral cochlear nucleus of the cat. J Neurophysiol 56:261–286.

Rhode WS, Oertel D, Smith PH. 1983. Physiological response properties of cells labeled intracellularly with horseradish peroxidase in cat ventral cochlear nucleus. J Comp Neurol 213:448–463.

Rietzel H-J, Friauf E. 1998. Neuron types in the rat lateral superior olive and developmental changes in the complexity of their dendritic arbors. J Comp Neurol 390:20–40.

Rouiller EM, Ryugo DK. 1984. Intracellular marking of physiologically characterized cells in the ventral cochlear nucleus of the cat. J Comp Neurol 225:167–186.

Ryan AF, Furlow Z, Woolf NK, Keithley EM. 1988. The spatial representation of frequency in the rat dorsal cochlear nucleus and inferior colliculus. Hear Res 36:181–189.

Saint Marie RL, Baker RA. 1990. Neurotransmitter-specific uptake and retrograde transport of [^{3}H]glycine from the inferior colliculus by ipsilateral projections of the superior olivary complex and nuclei of the lateral lemniscus. Brain Res 524:244–253.

Saint Marie RL, Morest DK, Brandon CJ. 1989. The form and distribution of GABAergic synapses on the principal cell types of the ventral cochlear nucleus of the cat. Hear Res 42:97–112.

Saldaña E, Lopez DE, Malmierca MS, Collia FP. 1987. Neuronal morphology of the ventral cochlear nucleus of the rat. A Golgi study. Acta Microsc 10:1–12.

Sanes DH, Friauf E. 2000. Development and influence of inhibition in the lateral superior olivary nucleus. Hear Res 147:46–58.

Sanes DH, Goldstein NA, Ostad M, Hillman DE. 1990. Dendritic morphology of central auditory neurons correlates with their tonotopic position. J Comp Neurol 294:443–454.

Scheibel ME, Scheibel AB. 1974. Neuropil organization in the superior olive of the cat. Exp Neurol 43:339–348.

Schofield BR, Cant NB. 1996. Origins and targets of commissural connections between the cochlear nuclei in guinea pigs. J Comp Neurol 375: 128–146.

Schwartz IR. 1992. The superior olivary complex and lateral lemniscal nuclei. In: Webster DB, Popper AN, Fay RR, editors. The mammalian auditory pathway: neuroanatomy. New York: Springer-Verlag. p 117–167.

Smith PH, Joris PX, Carney LH, Yin TC. 1991. Projections of physiologically characterized globular bushy cell axons from the cochlear nucleus of the cat. J Comp Neurol 304:387–407.

Smith PH, Joris PX, Yin TC. 1993. Projections of physiologically characterized spherical bushy cell axons from the cochlear nucleus of the cat: evidence for delay lines to the medial superior olive. J Comp Neurol 33:245–260.

Smith PH, Joris PX, Yin TC. 1998. Anatomy and physiology of principal cells of the medial nucleus of the trapezoid body (MNTB) of the cat. J Neurophysiol 79:3127–3142.

Spangler KM, Warr WB, Henkel CK. 1985. The projections of principal cells of the medial nucleus of the trapezoid body in the cat. J Comp Neurol 238:249–262.

Spirou GA, Brownell WE, Zidanic M. 1990. Recordings from cat trapezoid body and HRP labeling of globular bushy cell axons. J Neurophysiol 63:1169–1190.

Spirou GA, May BJ, Wright DD, Ryugo DK. 1993. Frequency organization of the dorsal cochlear nucleus in cats. J Comp Neurol 329:36–52.

Strominger NL. 1973. The origins, course and distribution of the dorsal and

intermediate acoustic stria in the rhesus monkey. J Comp Neurol 147:209–234.

Sullivan WE, Konishi M. 1984. Segregation of stimulus phase and intensity in the cochlear nucleus of the barn owl. J Neurosci 4:1787–1799.

Takahashi T, Moiseff A, Konishi M. 1984. Time and intensity cues are processed independently in the auditory system of the owl. J Neurosci 4:1781–1786.

Thompson AM. 1998. Heterogeneous projections of the cat posteroventral cochlear nucleus. J Comp Neurol 390:439–453.

Thompson AM, Thompson GC. 1987. Efferent projections from posteroventral cochlear nucleus to lateral superior olive in guinea pig. Brain Res 421:382–386.

Thompson AM, Thompson GC. 1991. Projections from the posteroventral cochlear nucleus to the superior olivary complex in guinea pig: light and EM observations with the PHA-L method. J Comp Neurol 303: 267–285.

Tolbert LP, Morest DK, Yurgelun-Todd DA. 1982. The neuronal architecture of the anteroventral cochlear nucleus of the cat in the region of the cochlear nerve root: horseradish peroxidase labelling of identified cell types. Neuroscience 7:3031–3052.

Tollin DJ, Yin TC. 2002a. The coding of spatial location by single units in the lateral superior olive of the cat. I. Spatial receptive fields in azimuth. J Neurosci 22:1454–1467.

Tollin DJ, Yin TC. 2002b. The coding of spatial location by single units in the lateral superior olive of the cat. II. The determinants of spatial receptive fields in azimuth. J Neurosci 22:1468–1479.

Tsuchitani C. 1977. Functional organization of lateral cell groups of the cat superior olivary complex. J Neurophysiol 40:296–318.

Tsuchitani C, Boudreau JC. 1966. Single unit analysis of cat superior olive S segment with tonal stimuli. J Neurophysiol 29:684–697.

Tsuchitani C, Boudreau JC. 1967. Encoding of stimulus frequency and intensity by cat superior olive S-segment cells. J Acoust Soc Am 42: 794–805.

Van Noort J. 1969. The structure and connections of the inferior colliculus. Assen: Van Gorcum and Company N.V.

Vater M, Feng AS. 1990. Functional organization of ascending and descending connections of the cochlear nucleus of horseshoe bats. J Comp Neurol 292:373–395.

Veenman CL, Reiner A, Honig MG. 1992. Biotinylated dextran amine as an anterograde tracer for single- and double-labeling studies. J Neurosci Methods 41:239–254.

Vetter DE, Mugnaini E. 1992. Distribution and dendritic features of three groups of rat olivocochlear neurons. Anat Embryol 185:1–16.

Vetter DE, Adams JC, Mugnaini E. 1991. Chemically distinct rat olivocochlear neurons. Synapse 7:21–43.

Viemeister NF. 1988. Psychophysical aspects of auditory intensity coding. In: Edelman GM, Gall WE, Cowan WM, editors. Auditory function: neurobiological bases of hearing. New York: Wiley. p 213–241.

Warr WB. 1966. Fiber degeneration following lesions in the anteroventral cochlear nucleus of the cat. Exp Neurol 14:453–474.

Warr WB. 1982. Parallel ascending pathways from the cochlear nucleus: Neuroanatomical evidence of functional specialization. In: Neff WD, editor. Contributions to sensory physiology. New York: Academic Press. p 1–38.

Warr WB, Beck JE. 1996. Multiple projections from the ventral nucleus of the trapezoid body in the rat. Hear Res 93:83–101.

Warr WB, Boche JB, Neely ST. 1997. Efferent innervation of the inner hair cell region: origins and terminations of two lateral olivocochlear systems. Hear Res 108:89–111.

White JS, Warr WB. 1983. The dual origins of the olivocochlear bundle in the albino rat. J Comp Neurol 219:203–214.

Yin TCT, Chan JCK. 1990. Interaural time sensitivity in medial superior olive of cat. J Neurophysiol 64:465–488.

Young ED, Shofner WP, White JA, Robert J-M, Voigt HF. 1988. Response properties of cochlear nucleus neurons in relationship to physiological mechanisms. In: Edelman GM, Gall WE, Cowan WM, editors. Auditory function: neurobiological bases of hearing. New York: Wiley. p 277–312.